Fuel 188 (2017) 121–131

Contents lists available at ScienceDirect

Fuel

journal homepage: www.elsevier.com/locate/fuel

Full Length Article

Low-temperature CO oxidation on Ag/ZSM-5 catalysts: Influence of Si/Al ratio and redox pretreatments on formation of silver active sites

E. Kolobova [a], A. Pestryakov [a,*], G. Mamontov [b], Yu. Kotolevich [c], N. Bogdanchikova [c], M. Farias [c], A. Vosmerikov [d], L. Vosmerikova [d], V. Cortes Corberan [e]

[a] Tomsk Polytechnic University, Tomsk 634050, Russia
[b] Tomsk State University, Tomsk 634050, Russia
[c] Centro de Nanociencias y Nanotecnología, UNAM, Ensenada 22860, Mexico
[d] Institute of Petroleum Chemistry, Siberian Branch, Russian Academy of Sciences, Tomsk 634055, Russia
[e] Institute of Catalysis and Petroleum Chemistry (ICP), CSIC, 28049 Madrid, Spain

HIGHLIGHTS

- Cationic Ag^{+} and $Ag_n^{\delta+}$ species are active sites in low temperature CO oxidation.
- An appropriate Si/Al ratio is essential for CO oxidation over supported Ag catalyst.
- Broensted acidity of zeolite correlates with the catalyst activity.
- Consecutive oxidizing and reducing pretreatments promote catalytic activity.
- Ag/ZSM-5 (80) catalyst displayed the highest activity in CO oxidation.

GRAPHICAL ABSTRACT

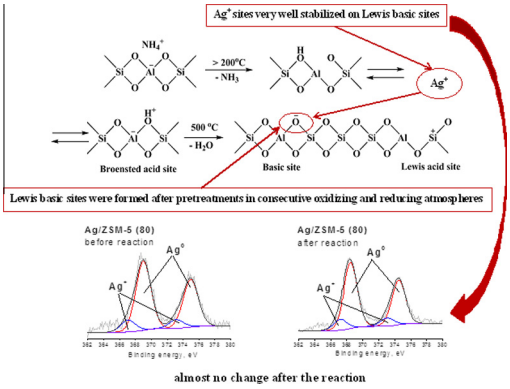

ARTICLE INFO

Article history:
Received 10 March 2016
Received in revised form 9 September 2016
Accepted 4 October 2016

Keywords:
Low temperature CO oxidation
Silver catalysts
ZSM-5
Si/Al ratio
Effect of pretreatments

ABSTRACT

Silver catalysts supported on ZSM-5 (Si/Al = 30, 50 and 80) were investigated for low-temperature CO oxidation to study the nature of the silver active sites and their formation under the influence of the support chemical composition and redox pretreatments. The catalysts were characterized by HRTEM, FTIR, XPS, diffuse reflectance UV–Vis spectroscopy, NH_3 thermodesorption (NH_3 TPD) and temperature-programmed reduction (H_2 TPR). The chemical composition (Si/Al ratio) of the ZSM-5 zeolite support significantly affects catalytic properties of Ag/ZSM-5 samples: the lower the Broensted acidity of the zeolite support, the higher the activity of the catalysts. Interestingly, while oxidizing pretreatment of catalysts led to a significantly better performance than reducing pretreatments, the consecutive reducing treatment of the preoxidized samples significantly promoted the catalytic activity for low-temperature CO oxidation. Thus, Ag/ZMS-5 catalyst with Si/Al = 80, pretreated consecutively in oxidizing and reducing conditions, showed the highest activity, reaching 90% CO conversion at just 40 °C. Comparison of activity and characterization results showed that silver particles with size below 2 nm are the most active; larger particles are just "spectators". The most probable silver active centers in the low-temperature CO oxidation are ionic species, mostly charged clusters $Ag_n^{\delta+}$, strongly interacting with the support. The obtained results in low-temperature CO oxidation might be of particular interest for neutralization of exhaust gases of car engines during "cold start".

* Corresponding author.
E-mail address: pestryakov2005@yandex.ru (A. Pestryakov).

http://dx.doi.org/10.1016/j.fuel.2016.10.037
0016-2361/

1. Introduction

The catalytic oxidation of carbon monoxide attracts considerable attention due to its relevance in many industrial sectors, such as gas cleaning in CO_2 lasers, CO sensors, air purification in devices for respiratory protection and protection of the environment from harmful emissions [1]. Development of catalysts of low-temperature CO oxidation is of particular interest for neutralization of exhaust gases of car engines during "cold start". Conventional car catalytic neutralizers based on Pt or Pd start to operate at 130–150 °C; and such differences between environmental and operating temperatures lead to emission of some amount of toxic exhaust gases to atmosphere.

Usually, catalysts containing noble metals (Pt, Pd, Rh, and Au) supported on transition metal oxides (Cr, Co, Cu, Ni, and Mn) [2–8] and hopcalite catalyst [9] are used in this process. The main drawbacks of catalysts containing noble metals are their high cost and the relatively high temperatures, above 100–120 °C, required for their efficient performance. Regarding hopcalite catalysts, their main drawback is deactivation by water vapor. By contrast, nanogold catalysts can operate at low temperatures (below 100 °C), but they are quickly deactivated during reaction or prolonged storage [6–8], and their cost is high. Consequently, there is the need to develop less expensive catalysts which possess both a high activity and stability.

Silver-containing catalytic systems are inferior in activity of supported gold, but more active than many oxide and metal catalytic systems [10,11]. The most important parameters influencing formation of the active species in silver-based catalysts are synthesis method, character of metal-support interaction, nature of the support, and redox pretreatments at different temperatures. All these factors predetermine the electronic state of supported silver, its dispersion and particle structure, and its catalytic properties. Concerning Ag-containing systems supported on silica and alumina, their thermal or reducing treatment with hydrogen-containing mixtures causes a reduction of silver from the ionic to the metallic state: the dispersed silver particles formed are active in oxidation reactions [12–14]. [AlO_4] tetrahedra are the centers of stabilization of ionic silver species in Ag/zeolite and Ag/aluminosilicate systems [15–18]. The dependence of the silver state on the surface of oxide supports of different nature on the pretreatment conditions and reaction mixtures has been described [19–21]. Silver dispersion on the TiO_2 surface is kept during treatments in inert and reducing atmosphere, whereas for Ag/Al_2O_3 the slight decrease of the metal dispersion is observed. Under the same conditions, aggregation of silver on the surface of SiO_2 is more pronounced; it causes loss of active surface due to dispersion decrease. Zhang et al. [22] discussed the influence of silver concentration on the catalytic activity and Ag particle size, as well as the effect of various pretreatments. Catalyst Ag/SiO_2 (8 wt.% Ag) pretreated with O_2 at 500 °C showed high catalytic activity in the CO oxidation (T_{98} = 65 °C). The further treatment with H_2 at 200 °C increased catalytic activity (T_{98} = 50 °C).

Catalysts supported on molecular sieves have also been investigated for low-temperature CO oxidation, especially those based on ZSM-5, due to their excellent thermal stability, high surface area and well developed preparation methods [23–26]. ZSM-5 is widely used fora variety of reactions, such as Fischer-Tropsch synthesis, deNO_x process and aromatization of hydrocarbons. Bi and Lu [24] studied catalyst Pd-Fe-O_x/NaZSM-5 in the low-temperature CO oxidation (T_{100} = 47 °C). Han et al. [25] prepared a series of Pd-Ce/ZSM-5 catalysts and found that the bicomponent Pd-Ce catalyst has higher activity for low-temperature CO oxidation than the Pd or Ce monometallic ones. In general, Pt or Pd-containing zeolites are the most studied for this process, while data on Ag/zeolite systems are much scarce [10]. Oleksenko et al. [26] investigated the catalytic activity of Ag-zeolite (10 wt.% Ag) systems calcined at high temperatures (up to 700 °C) and found that the additional reduction treatment of the samples leads to increase activity of Ag-NaX, Ag-NaA, Ag-NaZSM-5 (37), Ag-NaZSM-5 (47), and Ag-NaMor catalysts. The activity of these zeolite-based systems is largely determined by the number of active sites (Ag^0 clusters and highly dispersed metallic silver particles) which are formed during the preparation of catalysts and during the catalytic reaction.

Han et al. [25] also reported that increasing the Si/Al ratios leads to growth of the catalytic activity, but did not explain why ratio Si/Al influences the activity. Generally, the influence of Si/Al ratio of some zeolites (mordenites, Y, etc.) on physicochemical and catalytic properties of supported metal is caused by the correlation between their Si/Al ratio and surface acidity [8,9,27–31]. However, the mechanism of the effect of Si/Al ratio (and, accordingly, of surface acidity) on catalytic properties of the metals in redox processes remains unclear.

Despite the large number of publications devoted to the study of the mechanism of formation and the nature of active sites in the silver-containing systems, this question is still subject of broad discussion. Some authors suggest that the active sites are metallic silver particles of different sizes, while others prove the activity of ionic states [32–36]. The identification of the nature of the active sites is one of the key aspects of heterogeneous catalysis, because it allows carrying out the directed synthesis of highly efficient catalysts with desired properties.

In our previous study [37] we investigated and discussed the influence of the silver content and the synthesis conditions on the activity of zeolite supported silver catalysts for CO oxidation using a ZSM-5 zeolite with Si/Al = 50 as support. It was found that Ag/ZSM-5 catalysts have a good reproducibility and stability in CO oxidation and their activity depends strongly on Ag loading: the best performance was obtained with among which 7 wt.% Ag. The aim of this work is looking for ways to improve the activity of nanosized Ag catalysts to make them an alternative to nanogold catalysts for low temperature oxidation of CO. For this purpose, we investigated the nature of the silver active sites on the zeolite support surface, and how factors such as the chemical composition of the support (i.e., Si/Al ratio) and the pretreatment atmospheres influence their formation and redox properties.

2. Experimental

2.1. Catalysts preparation

All catalysts were prepared by incipient wetness impregnation of ZSM-5 zeolites in ammonium form with Si/Al ratios of 30, 50 and 80 (Süd-Chemie) with aqueous solution of $AgNO_3$ (0.1103 g/ml), by adding 1 ml of this solution per gram of support (this volume corresponds to internal pore volume of zeolite). Then, the obtained samples were dried at 150 °C for 3 h. Following our previous results [37], silver content in all samples was 7 wt.%. Support and catalyst samples were denoted ZSM-5 (*x*) and Ag/ZSM-5 (*x*), respectively, where *x* is the support Si/Al ratio.

2.2. Catalysts and supports characterization

IR spectra of studied zeolites were recorded on FTIR Nicolet 5700 spectrometer.

The porous structure of zeolites and catalysts was determined by N_2 low-temperature adsorption using 3Flex analyzer (Micromeritics, USA). Specific surface areas were calculated by

BET method in p/p^o range from 0.001 to 0.05 with positive value of constant. The micropores specific surface area and volume were calculated by t-plot and Horvath-Kawazoe methods. Pore size distributions were plotted according BJH-Desorption method (mesopores) and Horvath-Kawazoe (micropores, cylinder pore geometry). All samples (0.05–0.08 g) were degassed at 50 mtorr at 90 °C for 1 h and at 350 °C for 4 h. The acidic properties of the samples were studied by temperature programmed desorption of ammonia ($TPDNH_3$) according to a previously described method [38].

Catalyst samples were investigated by X-ray photoelectron spectroscopy (XPS) after treatment in hydrogen at 400 °C for 1 h with a SPECS custom made system using a PHOIBOS 150 WAL hemispherical analyzer and a μ-FOCUS 500 X-ray source. All the data were acquired using non-monochromated Al Kα X-rays (1486.6 eV, 200 W). A pass-energy of 50 eV, a step size of 0.1 eV/step and a high-intensity lens mode were selected. The diameter of the analyzed area was 3 mm. Charging shifts were referenced against adventitious carbon (C 1s at 284.5 eV). The pressure in the analysis chamber was maintained lower than 1×10^{-8} mbar. The accuracy of the BE values was ±0.1 eV. Peak intensities were estimated by calculating the integral of each peak after subtracting an S-shaped background and fitting the experimental peak to a combination of Lorentzian/Gaussian lines with variable proportions.

A JEOL-5300 scanning electronic microscope (SEM) was utilized for a general sample morphology observation. Silver contents were measured by energy dispersive spectroscopy (EDS) in the same system equipped with a Kevex Superdry detector.

High resolution transmission electron microscopy (HRTEM) studies were carried out using a JEM 2100F microscope operating with a 200 kV accelerating voltage. The samples after treatment in hydrogen at 400 °C for 1 h were ground into a fine powder and dispersed ultrasonically in hexane at room temperature. Then, a drop of the suspension was put on a lacey carbon-coated Cu grid. At least ten representative images were taken for each sample. Particle size distribution was obtained by counting ca. 100 particles for each sample.

Catalyst samples, either as-prepared or pretreated in consecutive oxidizing and reducing (O_2 at 600 °C for 1 h + H_2 at 400 °C for 1 h) atmospheres, were studied by diffuse reflectance UV–visible spectroscopy (DRS) with a Varian Cary 5000 spectrometer, in the wavelength range between 200 and 800 nm. $BaSO_4$ was used as a reference material. The percentage of reflectance was converted into f(R) values using the Kubelka–Munk transform. The spectra were collected at room temperature using samples ground into powder with no other pretreatment.

Temperature-programmed reduction (TPR) tests were carried out in a chemisorption analyzer «ChemiSorb 2750» (Micromeritics, USA) coupled with a mass spectrometer «UGA-300» (Stanford Research Systems). The samples (200 mg) were placed in a U-shaped reactor fed with 20 ml/min of gaseous mixture 10 % H_2/Ar and heated at a rate of 10 °C/min in the temperature range from −50 to 600 °C. Oxidative pretreatment of samples was conducted in temperature-programmed oxidation mode (TPO) in the air flow (20 ml/min) in the range from 25 to 600 °C (heating rate 10 °C/min), followed by keeping temperature at 600 °C for 20 min, and cooling under flowing air down to 25 °C (cooling rate 20 °C/min). The reaction/desorption products were monitored using mass spectrometry.

2.3. Catalytic CO oxidation

Catalytic tests in CO oxidation were carried out in a flow reactor using a gas mixture of 5% CO + 5% O_2 + 90% Ar (flow rate 200 ml/min). The weight of the catalyst sample was 1 g.

To study the influence of the atmosphere pretreatment on catalytic activity the catalyst samples were pretreated for one hour in either reducing (H_2 at 400 °C), oxidizing (O_2 at 600 °C), or consecutive oxidizing and reducing (O_2 at 600 °C + H_2 at 400 °C) atmospheres.

3. Results

3.1. Catalytic activity

The influence of the pretreatment atmosphere on the catalyst activity of Ag/ZM-5 catalysts with different Si/Al ratios is presented in Table 1. For each catalyst, activity varied depending on the pretreatment, increasing in the order: reduction (H_2) < oxidation (O_2) < consecutive oxidation + reduction ($O_2 + H_2$). Though oxidative pretreatment increased their catalytic activity as compared with those pretreated with reducing atmosphere, the best effect was achieved by reducing treatment of the preoxidized sample, i.e., by the combination of consecutive oxidation and reduction (ox-red) pretreatments. Many authors explained the pretreatment effects by the increase of amount of reactive oxygen species (O^{2-}, O^-, O_2^-) which favor CO oxidation on the support surface, as well as by formation of silver ions which play an important role in the genesis of high catalytic activity [22,39–42].

On the other hand, for samples submitted to the same pretreatment, catalytic activity increases significantly by increasing the Si/Al ratio. Fig. 1 clearly illustrates the effect of Si/Al ratio on the catalytic activity of samples pretreated consecutively in oxidative and reductive atmospheres. As a consequence, Ag/ZSM-5 (80) showed the highest activity in the CO oxidation after pretreatment in ox-red atmospheres (T_{50} = 37 °C or T_{90} = 40 °C), comparable to those reported by Zhang et al. [22]. This implies that the right selection of the support and the pretreatment of Ag/ZSM-5 catalysts can reduce by 140 °C the temperature needed to reach 90 % CO conversion, as compared with the least efficient one.

Cooling the reactor after the catalyst run showed some hysteresis of the light-off curves (Fig. 2). However, this effect was not pronounced. It indicates high stability of Ag active states during the reaction. Also, as was shown in our earlier studies, the studied catalytic systems are stable in CO oxidation for longer period [37].

3.2. Characterization of supports and catalysts

A series of physicochemical researches have been carried out to identify its possible influence on nature of the active sites, the conditions of their formation and stabilization.

3.2.1. IR spectra and BET results

IR spectra of all the ZSM-5 zeolites with different Si/Al ratios (Fig. 3) show absorption bands characteristic for high-silica zeolites. The absorption band at 550–560 cm^{-1}, characteristic for pentasyl type zeolites, is attributed to vibrations in the external bonds of the framework SiO_4 and AlO_4 tetrahedra; it indicates presence of twin 4, 5 and 6-membered rings [43]. Brønsted acidity is presented by vibrations of OH groups in the range 3000–3800 cm^{-1}. Intensity of these signals decreases with the increase of Si/Al ratio, as it could be expected due to the lower number of Al sites, in good correlation with results of NH_3 TPD (see below).

The BET surface area, pore volume and pore characteristics of micropores of the studied zeolites and Ag-containing catalysts are shown in Table 2, that summarizes isotherms of N_2 adsorption-desorption for zeolites (Fig. 4a). High values of sorption at low relative pressure (p/p^o < 0.05) for all samples evidenced the microporous structure of zeolite. In addition, presence of hysteresis loop in isotherms indicated presence of mesopores in zeolite, prob-

Table 1
Influence of redox pretreatments and support composition on activity of Ag/ZSM-5 catalysts for CO oxidation.

Si/Al ratio	Temperature of 50 % CO conversion (T_{50}), °C			Temperature of 90 % CO conversion (T_{90}), °C		
	H_2, 400 °C	O_2, 600 °C	O_2, 600 °C + H_2, 400 °C	H_2, 400 °C	O_2, 600 °C	O_2, 600 °C + H_2, 400 °C
30	125	117	100	180	120	105
50	98	80	75	110	85	80
80	78	59	37	85	65	40

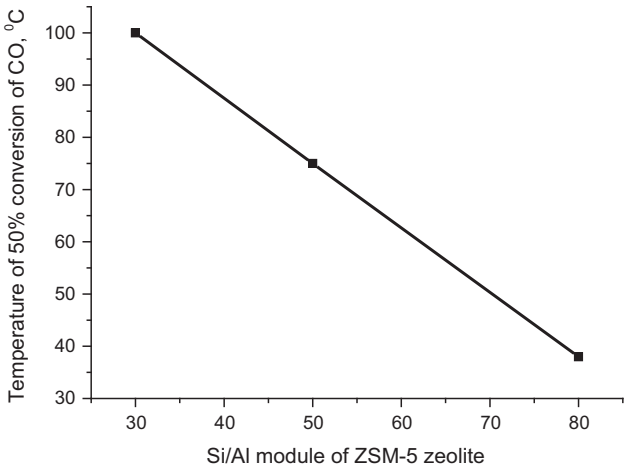

Fig. 1. CO oxidation on Ag/ZSM-5 catalysts after consecutive oxidation-reduction pretreatment: dependence of temperature for 50% CO conversion (T_{50}) on Si/Al ratio of the support.

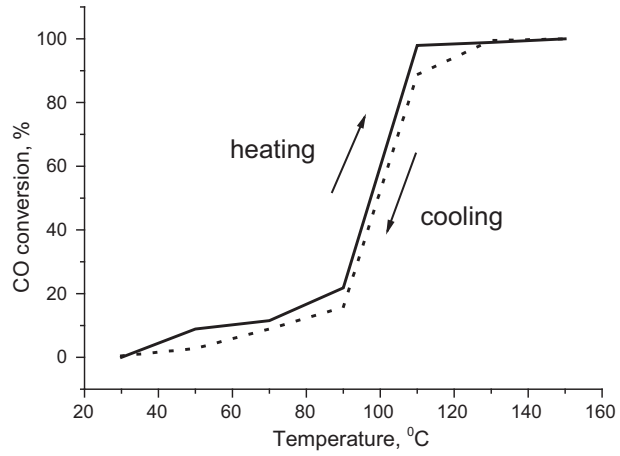

Fig. 2. Temperature cycle for Ag/ZSM-5 (50) catalyst after reduction pretreatment.

ably intra particle. To compare porosity of initial zeolites and Ag-containing catalysts the pore size distributions are presented in Fig. 4b–d for both micropores (Horvath-Kawazoe method) and mesopores (DJH-Desorption). All zeolites had similar specific surface areas, total pore volume and volume of micropores. Introduction of silver in porous structure of zeolites leads to insignificant decreasing of surface area and pore volume, which indicates part of supported silver located inside the pores of zeolites. Analysis of changes of surface areas of micro- and mesopores upon silver introduction, calculated by t-plot method (Table 2, S_{micro} and $S_{external}$), allows concluding that silver was predominantly inside micropores. In addition, there was no significant change of mesopores volume (Fig. 4b–d), while the decrease the average micropore width (Table 2) and the shift of micropore size distribution to small pore sizes after silver introduction indicates silver was deposited mostly inside pores with size of about 0.9 nm.

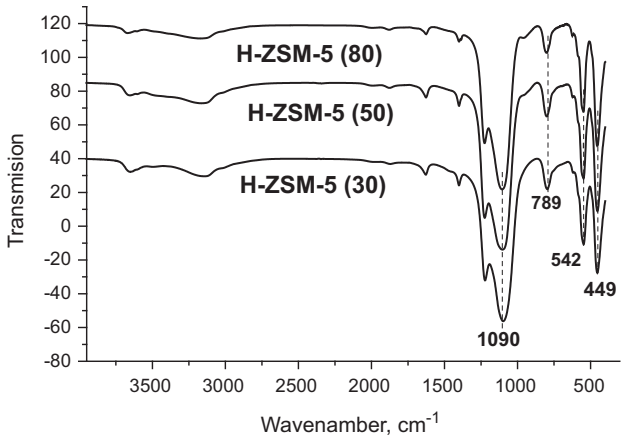

Fig. 3. IR spectra of the ZSM-5 zeolite supports with Si/Al = 30, 50 and 80.

3.2.2. TPD NH_3 results

The TPD NH_3 method was used to determine the acid properties of the initial zeolites, and catalysts based on them. Table 3 shows that only two types of acid sites, in forms I and III, were observed for the initial zeolites. Ascription of the low-temperature peak (form I) is not straightforward, as there are divergent points of view on the nature of acid sites associated with that peak. Some researchers suppose that this peak corresponds to the weakly acidic OH groups, but the majority of researchers attributed it to the adsorption of ammonia on non-acidic terminal Si—OH groups, similar to the silanol groups of silica belonging to both zeolites and impurities in zeolites such as, for instance, an amorphous phase [38]. Form III is associated with the adsorption of ammonia on the strong Brønsted acid sites (BAC), which belong to the zeolite [44,45]. With increasing Si/Al ratio a decrease in the concentration of acidic sites in the forms I and III was observed. After deposition of the silver and pretreatments in consecutive oxidizing and reducing atmospheres, new acidic sites in the forms II and IV are observed, where form II corresponds to Lewis acid sites (LAC) of the zeolite, formed in the dehydration process during the high temperature pre-treatment (Fig. 5), and form IV to LAC formed by coating silver due to the presence Ag^+ [46]. In addition, compared with the initial zeolites, a significant decrease in the concentration of BAC (form III) was observed for catalysts. This is due to the formation of Lewis basic centers from these BAC by the dehydration process under the influence of pre-treatment (Fig. 5). Ag^+ sites were localized and stabilized on these new LAC, whose concentration increased with increasing Si/Al ratio. This correlates well with the results of the catalytic tests: the best catalytic properties were observed for the catalyst with (support) ratio Si/Al = 80, that showed the highest concentration of Ag^+ (LAC).

3.2.3. HRTEM, EDX and XPS results

Elemental analysis showed quite similar Ag contents for all the catalysts (Table 4).

Fig. 6 shows representative micrographs and histograms of size distribution of the silver nanoparticles (Ag NPs) for the catalysts as

Table 2
The characteristics of porous structure of zeolites and Ag-containing catalysts.

Sample	S_{BET} (m^2/g)	Total pore volume (cm^3/g)	t-plot			Horvath-Kawazoe	
			S_{micro} (m^2/g)	$S_{external}$ (m^2/g)	V_{micro} (cm^3/g)	V_{micro} (cm^3/g)	W_{micro} (nm)
ZSM-5 (30)	426	0.273	315	112	0.127	0.174	0.852
ZSM-5 (50)	406	0.254	299	108	0.119	0.165	0.864
ZSM-5 (80)	438	0.253	298	140	0.120	0.179	0.870
Ag/ZSM-5 (30)	374	0.240	271	104	0.109	0.153	0.844
Ag/ZSM-5 (50)	390	0.256	284	106	0.114	0.158	0.840
Ag/ZSM-5 (80)	408	0.240	279	129	0.112	0.166	0.865

S_{micro}: micropore surface area; $S_{external}$: Specific surface area of meso- and macropores ($S_{micro} + S_{external} = S_{BET}$); V_{micro}: micropore volume; W_{micro} - average width of micropores.

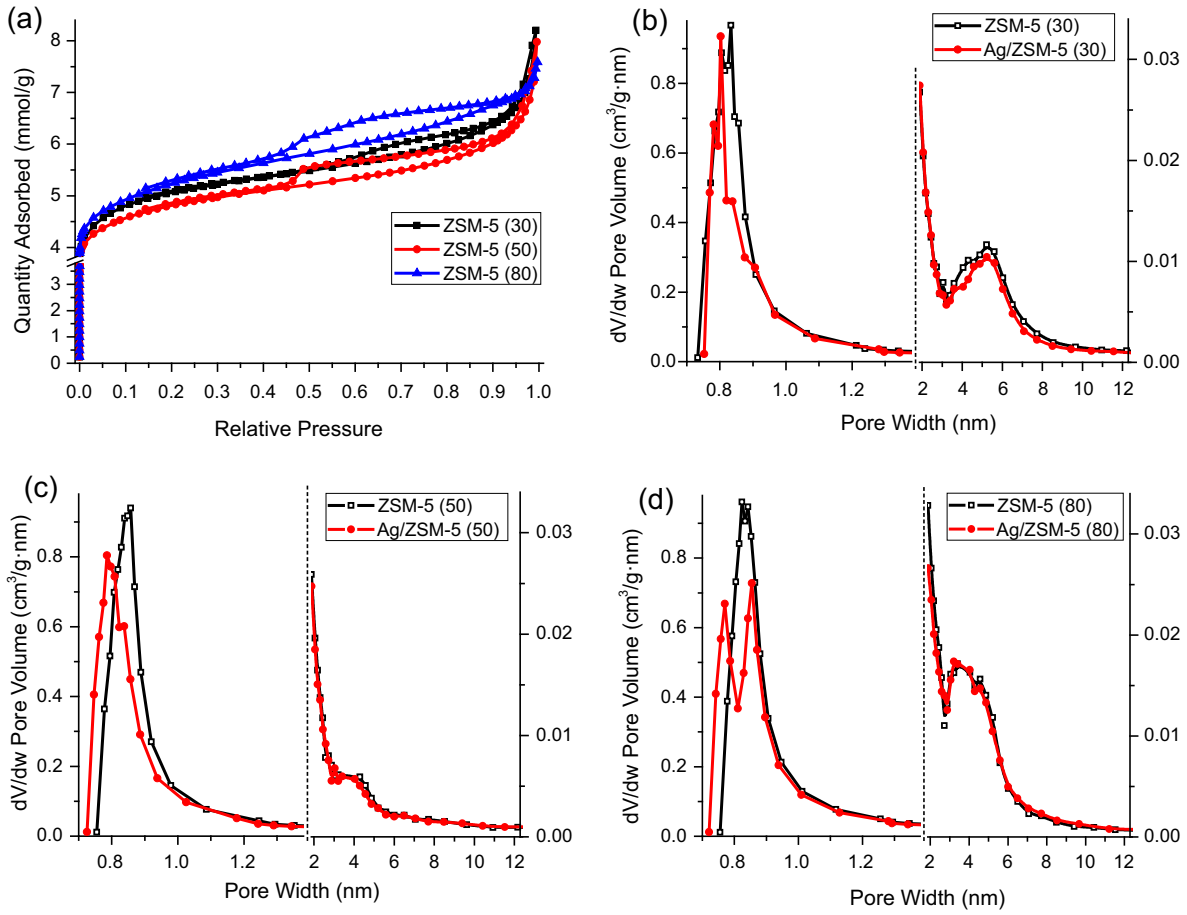

Fig. 4. N_2 adsorption-desorption isotherms for zeolites (a) and pore size distributions obtained by Horvath-Kawazoe (0.7–1.4 nm) and BJH-Desorption (1.8–13 nm) methods for zeolites and Ag/ZSM-5 catalysts with Si/Al ratios: 30 (b), 50 (c) and 80 (d).

Table 3
The acid properties of ZSM-5 zeolites and Ag-containing catalysts with different Si/Al ratio according to TPD NH_3.

Sample	$T_{max.}$, °C				Concentration of acid sites, μmol/g				
	T_I	T_{II}	T_{III}	T_{IV}	C_I	C_{II}	C_{III}	C_{IV}	$C_{\sum}$
H-ZSM – 5 (30)	200	–	430	–	496	–	348	–	844
H-ZSM – 5 (50)	200	–	405	–	416	–	201	–	617
H-ZSM – 5 (80)	185	–	400	–	408	–	188	–	596
Ag/ZSM – 5 (30)	180	280	455	550	325	383	87	66	861
Ag/ZSM – 5 (50)	155	250	410	505	204	310	64	74	652
Ag/ZSM – 5 (80)	140	240	400	540	135	231	60	93	519

T_I, T_{II}, T_{III}, T_{IV} – temperature of the peak maxima for forms I, II, III and IV; C_I, C_{II}, C_{III}, C_{IV} and $C_{\sum}$ - concentration of acidic sites in the forms I, II, III, IV and total, respectively.

a function of Si/Al ratio of the support, before (Fig. 6a, c and e) and after (Fig. 6b, d and f) their use in CO oxidation. From them it becomes evident that the average size of the silver particles is regulated by the chemical composition of the support; in this case, by the Si/Al ratio in the zeolite. The particle size distribution was significantly narrowed with the increase of Si/Al ratio. After the cat-

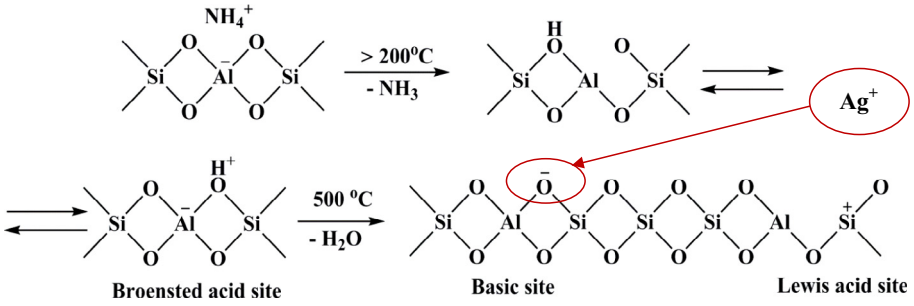

Fig. 5. Modification of the surface acid-base properties of the zeolites as a function of thermal treatment.

Table 4
Silver content in the studied catalysts.

Sample	Ag content, wt.%
Ag/ZSM – 5 (30)	4.9
Ag/ZSM – 5 (50)	4.7
Ag/ZSM – 5 (80)	5.2

alytic process only a slight change in the particle distribution range was observed for Ag/ZSM-5 (50) and Ag/ZSM-5 (80) samples. In contrast, significant changes of the particle size distribution for Ag/ZSM-5 (30) were observed after reaction: metal nanoparticle aggregation was very pronounced. It is also interesting to note that only for Ag/ZSM-5 (80) sample most of the particles had sizes <2 nm. Such small clusters may be considered as the most active sites of silver for the studied process [37,47].

XPS was used for study of the silver electronic state in the most active catalyst, Ag/ZSM-5 (80), and its change after the oxidation of CO. It should be noted that before the test the samples were pre-reduced at T = 400 °C, and reduction of silver may also take place under the influence of the X-ray beam; therefore, it should be expected that most of the silver will be in the reduced state. Ag3d XPS spectra (Fig. 7) show that either before and after the reaction silver on the surface of the zeolite is in two states with binding energies (BE) E_b ($Ag3d_{5/2}$) = 368.5–369 eV and E_b ($Ag3d_{5/2}$) = 367.2–367.3 eV. The former, due to the presence of small clusters of silver, has been observed for the highly dispersed particles of metal deposited on oxide supports (it can be shifted to higher binding energies range of up to 1–2 eV [48]). The latter corresponds to the Ag^+ ion. Analysis of the spectra shows that this ionic state was very resistant to the reaction media, there was practically no change in the metal/ion ratio after the catalytic process.

3.2.4. UV–vis spectroscopy

UV–Vis method was used to assess the influence of the atmosphere of pretreatment on the electronic state of silver depending on the chemical composition of the support. Fig. 8 shows UV–Vis spectra of as-prepared Ag/ZSM-5 catalysts (a) and after consecutive oxidation and reduction pretreatment (b). The absorption band at 310 nm for the as-prepared samples is attributed to large aggregates and a surface film of silver (electron interzonal transitions and intrinsic photo effect) [49]. It should be noted that for the sample with the ratio Si/Al = 30 the intensity of this absorption is maximum.

Several absorption bands not typical for the as-prepared sample were observed in the UV–vis spectra (Fig. 8b) after consecutive pretreatment of the catalysts in oxidizing and reducing atmospheres: the absorbance at 217 nm is assigned to $4d^{10}$–$4d^9 5s^1$ transitions in Ag^+; absorption in the ranges 270–290 nm and 368–392 nm corresponds to a charge transfer band in clusters $Ag_n^{\delta+}$ (n = 2–7) [49]. In addition, the absorption in the range of 368–392 nm, specifically related to clusters of silver up to 3 nm, is maximal for sample with Si/Al = 80, in good agreement with the TEM data (Fig. 6). Stable absorption band at 315 nm was observed only for Ag/ZSM-5 (30) sample; as mentioned above, this absorption refers to the large aggregates and a surface film of silver. As intensity of this absorption increased after pre-treatment, it may be associated with the aggregation of silver particles. These data also correlate well with the results of TEM (Fig. 6), as the proportion of large particles (>10 nm) is the highest only for this sample. Signal plasmon resonance (450–470 nm) of the respective metallic particles of a certain size was not observed in the spectra.

3.2.5. TPR results

Fig. 9a shows the TPR profiles obtained for freshly prepared samples. Two peaks are observed for all samples in the temperature range 120–220 °C, the second one appearing just as a shoulder for the Ag/ZSM-5 (30) sample, and they are shifted to higher temperatures with the increase of Al content. Emission of nitric oxides, observed by gas mass-spectrometry in this temperature range, confirmed the reduction of silver nitrate. Thus, for freshly prepared samples the silver reduction proceeds characteristically from silver nitrate.

Fig. 9b shows the TPR profiles of the samples after oxidative pretreatment at 600 °C. For all catalysts the significantly lower intensity of the hydrogen consumption (by one order of magnitude) was observed, as compared with the as-prepared samples (Fig. 9a). It is important to note that reduction of the various silver entities occurs at different reduction temperatures. After the oxidation treatment insignificant emission of NO_x and CO_2 (data not shown) was observed during TPR; thus, silver nitrate and carbonate were practically decomposed during the oxidation pretreatment.

The most intense hydrogen consumption was observed in the temperature range 40–250 °C. The peak at 83 °C results from reduction of dispersed silver oxides [50,51] and at 152–183 °C also associated with reduction of dispersed silver oxides and undecomposed silver nitrate. The peak at 83 °C increased with the increase of Si/Al ratio. This may be associated with an increasing portion of dispersed silver oxide on the surface of catalyst.

For catalysts with the higher Si/Al ratios several hydrogen consumption peaks appeared at higher temperatures, whose intensity increased with the increase of Si/Al. These peaks (with maxima at 350 and 440 °C) were attributed to reduction of silver ions strongly interacting with the support [52]. It should be noted that a hydrogen consumption peak at 570 °C was observed only for sample Ag/ZSM-5 (30) (its presence was also observed by mass spectrometry and in duplicated experiments) while there were not peaks with maximum at 350 and 440 °C for this sample.

Thus, during the oxidative treatment most of silver (50–60 %) went to metal state as a result of thermal decomposition of silver nitrate. However, TPR data indicate that part of silver was in the

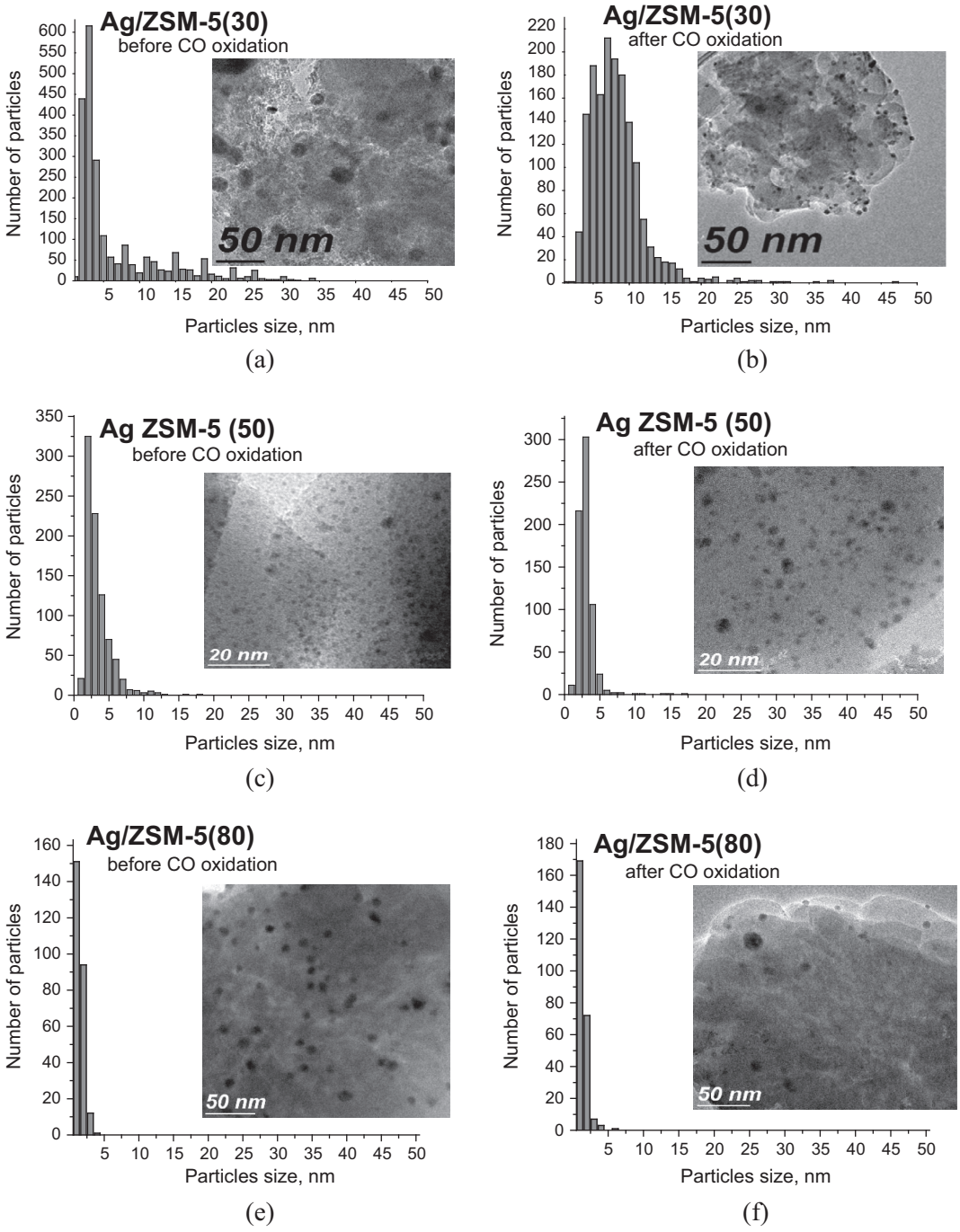

Fig. 6. Representative TEM micrographs and particle size distribution for Ag/ZSM-5 samples before (left column) and after (right column) their use in CO oxidation.

charged state in several forms: dispersed silver oxides (peaks at low temperatures), as well as ionic (perhaps, clustered) forms strongly interacting with the support (peaks at above 300 °C). Growth of the amount of oxidized silver and significant increase of cluster and ionic forms of silver are observed with the increase of Si/Al ratio. The peak at 570 °C in the TPR pattern of the sample Ag/ZSM-5 (30) is probably explained by reduction of specific silver ions or clusters strongly bonded with support.

4. Discussion

What are the reasons for the observed differences in activity of the samples with different Si/Al ratios after different pretreatments? Obviously, the nature and amount of the formed active sites are regulated by the chemical composition of the support and the conditions of pretreatment. Analysis of literature data [15–31] suggests a number of factors determining the sample activity: (a) structure of the support; (b) surface acidity of zeolite; (c) size of silver nanoparticles; (d) electronic state of the supported metal and its stability during the treatment.

The nature of the support and the pretreatment atmosphere are very important factors affecting the catalyst activity (which, in turn, is determined by the structural and electronic properties of the supported metal). The impact of these factors has been repeatedly discussed in the literature; however, there is no ~~a~~ consensus concerning influence of these factors on the formation of active

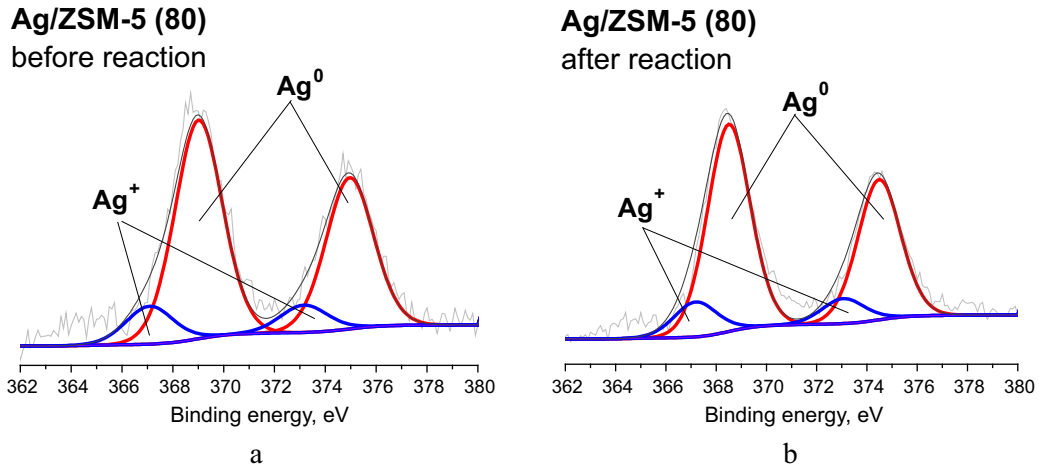

Fig. 7. XPS Ag3d peak of catalyst Ag/ZSM-5 (80) before (a) and after (b) use in CO oxidation.

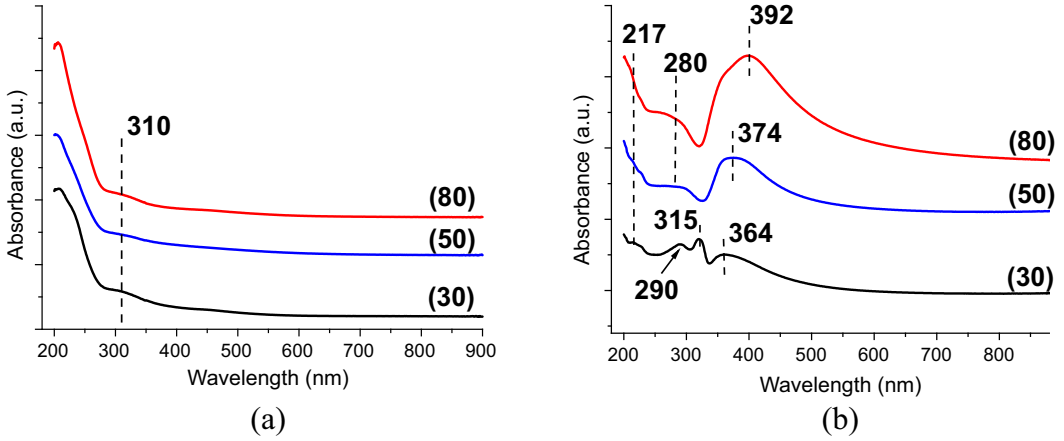

Fig. 8. UV–vis spectra of Ag/ZSM-5 catalysts with different zeolite Si/Al ratio (30, 50 and 80): without any pretreatment (a) and after consecutive oxidation and reduction pretreatments (b).

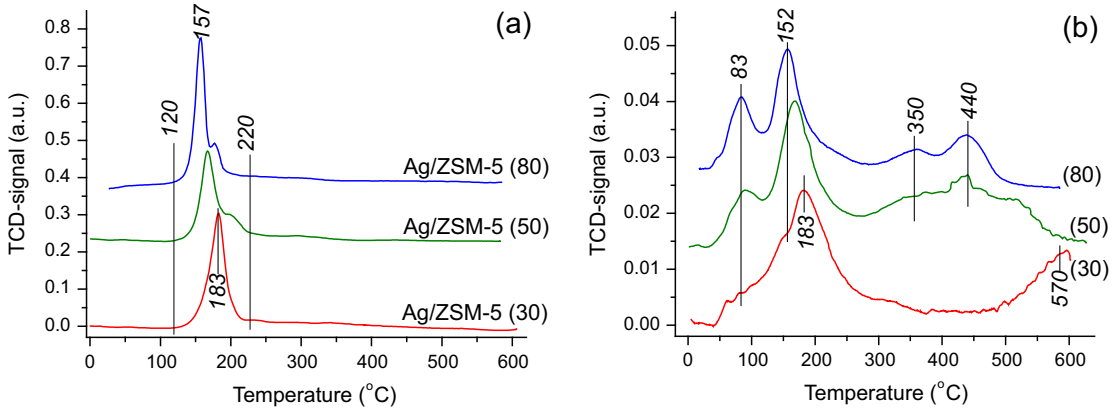

Fig. 9. TPR profiles for Ag/ZSM-5 catalysts as-prepared (a) and after oxidative pretreatment at 600 °C (b).

sites. Adsorption studies revealed a correlation between the CO oxidation activity of the catalyst and surface acidity of the zeolite [26]. However, as mentioned above, the acid sites themselves do not exhibit intrinsic catalytic activity because pure zeolite is not active in the studied reaction. Obviously, the proton acid sites influence the formation of active states of supported silver, in particular, the size of the metal nanoparticles and their electronic state.

According to the TPD NH_3 results (Table 3) after deposition of silver and pretreatment in consecutive oxidizing and reducing atmosphere, new acidic sites in the forms II and IV were observed, where form II is a Lewis acid site (LAC) of the zeolite formed in the

course of dehydration process during the high temperature pre-treatment, and form IV is LAC formed by coating silver due to the presence of Ag^+ ions. In addition, compared with the initial zeolites for catalysts, there is a significant decrease in the concentration of BAC (form III), due to the formation of the basic Lewis centers from BAC during the dehydration under the influence of pre-treatment, on them Ag^+ sites are localized and stabilized (Fig. 5), the concentration of these sites increases with increasing Si/Al ratio.

The presence of ionic sites of silver in the samples after pre-treatments, also confirmed by the TPR, UV–vis and XPS spectroscopy data was observed.

Treatment of the catalyst with hydrogen led to relatively weak activity at low-temperature (<100 °C), which implies, consequently, the formation of small amounts of the active sites. TPR data (Fig. 9) showed that all as-prepared samples are characterized by a slight reduction of silver from silver nitrate; for all samples two reduction peaks in the temperature range 120–250 °C were observed.

A significant increase in activity in the CO oxidation was observed after treating the catalyst in oxygen atmosphere. High-temperature oxidation treatment led to the formation of several states of the metal on the support surface, as identified by TPR (Fig. 9), XPS (Fig. 7) and UV–vis (Fig. 8). It gives rise to several low temperatures hydrogen consumption peaks, at 83 °C and a double peak at 152–183 °C, which are associated with the reduction of the dispersed silver oxides. Contribution of this double peak increased with the increase of Si/Al ratio. In addition, new hydrogen consumption peaks arise in high temperatures range (with maxima at 345 and 440 °C); their intensities increased with the Si/Al ratio. These peaks are attributed to reduction of silver ions strongly interacting with the support. Formation of clusters $Ag_n^{\delta+}$ in these samples was also revealed by UV–vis (Fig. 8, absorption in the range 270–290 nm and 368–392 nm). It should be noted that for the sample with the ratio of Si/Al = 80 the intensity of the absorption is maximum, it also agrees well with the TPR. The appearance of another high-temperature peak with maximum at 570 °C, observed only for sample Ag/ZSM-5 (30), indicates an interaction between silver and support stronger than in Ag/ZSM-5 (50) and Ag/ZSM-5 (80) samples. Probably, by virtue of this interaction, these centers cannot actively participate in the catalytic process at low temperatures. This type of centers could be formed by interaction of silver atoms with isolated aluminum cations expelled to extra framework positions during deep dehydration, as these centers are capable to strong electron-acceptor interactions. The higher aluminum content of this sample could have favored this expelling of aluminum out of framework.

It should be noted that for the most active Ag/ZSM-5 (80) sample, no change of the of metal/ion ratio in the XP spectra (Fig. 7) was observed after the catalytic process, what indicates good stabilization of Ag^+ sites in this sample.

Obviously, electronic state of silver plays a key role in its catalytic performance and the size of the metal particles is also directly related to electronic state, because highly dispersed particles are more easily oxidized and interact more strongly with the support. Investigation of silver particles size by TEM showed very interesting results.

According to TEM data, Ag NPs sizes of most samples are within a narrow range of 1–4 nm (Fig. 6). Absence of XRD signals of metallic silver in catalysts' diffractograms (not shown) also confirms the high dispersion of the metal particles. Work in the catalytic process has little effect on particle size distribution excepting for the sample Ag/ZSM-5 (30), where this effect is significant. Furthermore, it is evident that the average size of the silver particles is highly dependent on the nature of the support. With increasing Si/Al ratio the particle size distribution is considerably narrowed in parallel with the increase in activity. Obviously, silver also displays activity in the low-temperature oxidation reactions only in highly dispersed state. As it has been shown previously for a number of gold catalysts, only particles with size of 1 nm or less are active in CO oxidation [8,9,53–59]. Part of these highly dispersed clusters are not detectable by TEM and XRD, but can be observed in UV–Vis spectra [55–59]. The comparison of the activity results with the particle size distribution in the three silver catalysts allows suggesting that particles with size <2 nm to be the most active states; the larger particles are probably just "spectators" or much less active. In addition, according to the BET (Table 2, Fig. 4), the part of silver located inside the micropores of zeolite, has a particle size of less than 0.9 nm.

According to the physicochemical and catalytic results, Ag/ZSM-5 (80) catalyst has the higher concentration of Ag^+ states and the highest catalytic activity among the investigated samples. In turn, the activity is determined by the effective stabilization of the ionic silver on the zeolite surface, which is achieved by selecting of the optimal Si/Al ratio and optimum pretreatment. Obviously, during preparation Brønsted acid sites hinder stabilization of ionic silver in strongly bound forms on the surface of the zeolite. When silver is supported on zeolite by ion-exchange method proton sites promote stabilization of metal. But, as we used water capacity impregnation method, the surface protons, by contrast, may compete with the silver ions; therefore, stabilization of the ionic form can only be achieved by an additional pre-treatment, oxidizing-reducing pre-treatment in our case, which will help to reduce the concentration of BAC. The oxidizing treatment leads to: (1) decomposition of silver precursor on the zeolite surface with the formation of several silver states: metallic, ionic and cluster; (2) dehydration of the zeolite surface and formation of the basic Lewis centers from BAC, Ag^+ states are localized and stabilized on them; (3) formation of the adsorbed oxygen species promoted the oxidation process. Then the subsequent ~~a~~ reducing treatment probably reduces partially the ionic silver, forming the optimal effective charge δ^+ ($0 < \delta^+ < 1$). It has been reported than on silver catalysts the selective oxidation of alcohols is carried out on the active centers with the maximum effective charge, but complete oxidation is carried out on the active centers with minimum effective charge [44,60]. Qu et al. [19] reported that the subsequent reducing treatment leads to a partial aggregation of silver nanoparticles with the formation of defective particles, in which the adsorption of CO and oxygen is easier and faster than on non-defective particles.

Thus, the obtained results allow suggesting silver ionic states, mostly charged clusters $Ag_n^{\delta+}$ strongly interacting with the support, to be the active sites of silver in the low-temperature CO oxidation. The size of these clusters is probably lower than 2 nm.

Nevertheless, it should be noted that researches proving the activity of metallic (uncharged) species of silver do not contradict this statement. Silver can be in uncharged state in the initial catalysts. However, it is known that CO is not adsorbed on Ag^0 at room temperature [36,37,61,62]. Therefore, for starting the reaction it is necessary, in any case, the adsorption of oxygen, which leads to formation of the ionic silver form. Any factors favoring the formation of these ionic species will promote the process. If such ionic forms (e.g., clusters $Ag_n^{\delta+}$) are already present in the initial sample, the catalyst reacts more rapidly and displays activity at lower temperatures.

5. Conclusions

Chemical composition (Si/Al ratio) of ZSM-5 zeolite supports significantly affects catalytic properties of Ag/ZSM-5 catalysts for CO oxidation. Decreasing the Brønsted acidity of zeolite correlates with the increase of catalytic activity, what indicates that Brønsted

acid sites hinder stabilization of ionic silver in strongly bound forms on the surface of the zeolite. Redox pretreatments significantly modify the catalytic performance, because of decrease of BAC concentration by their transformation into Lewis basic centers, on which ionic silver is localized and stabilized. Interestingly, while single oxidative pretreatment leads to better activity than direct reduction pretreatment, the best performance is showed when the preoxidized catalyst is then reduced prior to catalytic tests. The analysis of evolution of silver species during TPR experiments and of the catalysts after such pretreatments by UV–vis spectroscopy has allowed to identify the nature of the different types of silver species (metallic, ionic, clusters) present in the catalysts, showing that the most probable silver active centers in the low-temperature CO oxidation are ionic states, mostly charged clusters $Ag_n^{\delta+}$ strongly interacting with the support. Comparison of the silver particle size distribution determined from HRTEM with catalytic activity data demonstrate that the most active silver particles have sizes smaller than 2 nm; the larger particles are just "spectators" or much less active.

These results evidence that the proper selection of the support composition and the redox pretreatment can greatly improve the activity of these Ag-based catalysts for low temperature CO oxidation. Thus, Ag/ZMS-5 catalyst with Si/Al = 80, pretreated consecutively in oxidizing and reducing conditions, showed the highest activity, reaching 90% CO conversion at just 40 °C. This indicates alternative ways to improve the performance of Ag-based catalysts as lower cost catalysts for CO oxidation.

The obtained results in low-temperature CO oxidation might be of particular interest for neutralization of exhaust gases of car engines during "cold start".

Acknowledgements

This research was supported by CONACYT project 260409 and PAPIIT-UNAM projects IT200114, IN105114 and IN107715 (Mexico) and by Government Program «Science» of Tomsk Polytechnic University, Grant No. 4.1187.2014/K.

References

[1] Farrauto RJ, Heck RM. Environmental catalyst of the 21st century. Catal Today 2000;55:179–87.
[2] Scirè S, Minicò S, Crisafulli C, Satriano C, Pistone A. Catalytic combustion of volatile organic compounds on gold/cerium oxide catalysts. Appl Catal B: Environ 2003;40:43–9.
[3] Wang W, Zhang HB, Lin GD, Xiong ZT. Study of $Ag/La_{0.6}Sr_{0.4}MnO_3$ catalysts for complete oxidation of methanol and ethanol at low concentrations. Appl Catal B: Environ 2000;24:219–32.
[4] Spivey JJ, Butt JB. Literature review: deactivation of catalysts in the oxidation of volatile organic compounds. Catal Today 1992;11:465–500.
[5] Kolobova E, Kotolevich Y, Pakrieva E, Mamontov G, Farías MH, Bogdanchikova N, Cortés Corberán V, Pestryakov A. Causes of activation and deactivation of modified nanogold catalysts during prolonged storage and redox treatments. Molecules 2016;21:486.
[6] Haruta M, Yamada N, Kobayashi T, Iijima S. Gold catalysts prepared by coprecipitation for low-temperature oxidation of hydrogen and of carbon monoxide. J Catal 1989;115:301–9.
[7] Hashmi ASK, Hutchings GJ. Gold catalysis. Angew Chem Int Ed 2006;45:7896–936.
[8] Bond GC, Louis C, Thompson DT. Catalysis by gold. London: Imperial College Press; 2006.
[9] Fierro G, Morpurgo S, Jacono ML, Inversi M, Pettiti I. Preparation, characterisation and catalytic activity of Cu-Zn-based manganites obtained from carbonate precursors. Appl Catal A 1998;166:407–17.
[10] Zhang X, Qu Z, Yu F, Wang Y. Progress in carbon monoxide oxidation over nanosized Ag catalysts. Chin J Catal 2013;34:1277–90.
[11] Kotolevich Y, Kolobova E, Khramov E, Cabre-ra JE, Farías MH, Zubavichus Y, Zanella R, Mota-Morales JD, Pestryakov A, Bog-danchikova N, Cortés Corberán V. Identification of subnanometric Ag species, their interaction with supports and role in catalytic CO oxidation. Molecules 2016;21(4):532–49.
[12] Mamontov GV, Dutov VV, Sobolev VI, Vodyankina OV. Effect of transition metal oxide additives on the activity of an Ag/SiO_2 catalyst in carbon monoxide oxidation. Kinet Catal 2013;54:487–91.
[13] Sotiriou GA, Teleki A, Camenzind A. Nanosilver on nanostructured silica: antibacterial activity and Ag surface area. J Chem Eng 2011;170:547–54.
[14] Scire S, Minico S, Crisafulli C, Galvagno S. Catalytic combustion of volatile organic compounds over group IB metal catalysts on Fe_2O_3. Catal Commun 2011;2:229–32.
[15] Sarkar DK, Clouter F, El Khakani MA. Electrical switching in sol-gel derived Ag-SiO_2 nanocomposite thin films. J Appl Phys 2005;97(084302):1–5.
[16] Dai WL, Li JL, Cao Y, Liu Q, Deng JF. Novel sol–gel-derived Ag/SiO_2–Al_2O_3 catalysts for highly selective oxidation of methanol to formaldehyde. Catal Lett 2000;64:37–40.
[17] Dai WL, Cao Y, Ren LP, Yang XL, Xu JH, Li HX, He HY, Fan KN. Ag–SiO_2–Al_2O_3 composite as highly active catalyst for the formation of formaldehyde from the partial oxidation of methanol. J Catal 2004;228:80–91.
[18] Lippits MJ, Boerlwema RRH, Neiuwenhuys BE. A comparative study of oxidation of methanol on γ-Al_2O_3 supported group IB metal catalysts. Catal Today 2009;145:27–33.
[19] Qu Z, Huang W, Cheng M, Bao X. Restructuring and redispersion of silver on SiO_2 under oxidizing/reducing atmospheres and its activity toward CO oxidation. J Phys Chem B 2005;109:15842–8.
[20] Qu Z, Huang W, Cheng M, Bao X. Formation of subsurface oxygen species and its high activity toward CO oxidation over silver catalysts. J Catal 2005;229:446–58.
[21] Dorofeeva HB, Knyazev AC, Radishevskaya NI, Salanov AN, Shilyaeva LP, Sudakova NN, Vodyankina OV. Specifics of the desorption of oxygen from a silver surface promoted by phosphates. Rus J Phys Chem 2007;81:788–93.
[22] Zhang X, Qu Z, Li X, Wen M, Quan X, Ma D, Wu J. Studies of silver species for low-temperature CO oxidation on Ag/SiO_2 catalysts. Sep Purif Technol 2010;72:395–400.
[23] Konova P, Arve K, Klingstedt F, Nikolov P, Naydenov A, Kumar N, Murzin DYu. A combination of Ag/alumina and Ag modified ZSM-5 to remove NO_x and CO during lean conditions. Appl Catal B: Environ 2007;70:138–45.
[24] Bi YS, Lu GX. Catalytic CO oxidation over palladium supported NaZSM-5 catalysts. Appl Catal B 2003;41:279–86.
[25] Han W, Zhang P, Tang Z, Lu G. Low temperature CO oxidation over Pd–Ce catalysts supported on ZSM-5 zeolites. Process Saf Environ Prot 2014;92:822–7.
[26] Oleksenko LP, Yatsimirskiy VK, Chen Y, Lutsenko L. The activity of Ag-containing zeolite catalysts in the oxidation reaction. Ukrainian Chem J 2008;74:42–6.
[27] Simakov A, Tuzovskaya I, Bogdanchikova N, Pestryakov A, Avalos M, Farías M, Lima E. Influence of sodium on activation of gold species in Y–zeolites. E Catal Commun 2008;9:1277–81.
[28] Smolentseva E, Bogdanchikova N, Simakov A, Pestryakov A, Avalos M, Farias MH, Tompos A, Gurin V. Catalytic activity of gold nanoparticles incorporated into modified zeolites. J Nanosci Nanotechnol 2007;7:1882–6.
[29] Pestryakov A, Tuzovskaya I, Smolentseva E, Bogdanchikova N, Jentoft F, Knop-Gericke A. Formation of gold nanoparticles in zeolites. Int J Mod Phys B 2005;19:2321–6.
[30] Pestryakov A, Bogdanchikova N, Simakov A, Tuzovskaya I, Jentoft F, Farias M, Diaz A. Surf Sci 2007;601:3792–5.
[31] Simakov A, Tuzovskaya I, Pestryakov A, Bogdanchikova N, Gurin V, Avalos M, Farías MH. On the nature of active gold species in zeolites in CO oxidation. Appl Catal A: Gen 2007;331C:121–8.
[32] Flura A, Can F, Courtois X, Royer S, Duprez D. High-surface-area zinc aluminate supported silver catalysts for low-temperature SCR of NO with ethanol. Appl Catal B: Environ 2012;126:275–89.
[33] Bechoux K, Marie O, Daturi M, Delahay G, Petitto C, Rousseau S, Blanchard G. Infrared evidence of room temperature dissociative adsorption of carbon monoxide over Ag/Al_2O_3. Catal Today 2012;197:155–61.
[34] Zhen-Zhen Q, Yu Y, Jian-Guo M. Adsorption of carbon monoxide on Ag(I)-ZSM-5 zeolite: an *ab initio* density functional theory study. Appl Surf Sci 2012;258:9629–35.
[35] Wichterlova B, Sazama P, Breen JP, Burch R, Hill CJ, Čapek L, Sobalík Z. An in situ UV–vis and FTIR spectroscopy study of the effect of H_2 and CO during the selective catalytic reduction of nitrogen oxides over a silver alumina catalyst. J Catal 2005;235:195–200.
[36] Hadjiivanov KI. IR study of CO and NOx sorption on Ag-ZSM-5. Micropor Mesopor Mater 1998;24:41–9.
[37] Kolobova E, Pestryakov A, Shemeryankina A, Kotolevich Y, Martynyuk O, Tiznado Vazquez HJ, Bogdanchikova N. Formation of silver active states in Ag/ZSM-5 catalysts for CO oxidation. Fuel 2014;138:65–71.
[38] Vosmerikov AV, Erofeev VI. Effect of mechanical treatment on the catalytic properties of zeolite catalysts for aromatization of lower alkanes. Rus J Phys Chem 1995;69:787–90.
[39] Yu L, Shi Y, Zhao Z, Yin H, Wei Y, Liu J, Kang W, Jiang T, Wang A. Ultrasmall silver nanoparticles supported on silica and their catalytic performances for carbon monoxide oxidation. Catal Commun 2011;12:616–20.
[40] Afanasev DS, Yakovina OA, Kuznetsova NI, Lisitsyn AS. High activity in CO oxidation of Ag nanoparticles supported on fumed silica. Catal Commun 2012;22:43–7.
[41] Zhang X, Qu Z, Li X, Zhao Q, Wang Y, Quan X. Low temperature CO oxidation over Ag/SBA-15 nanocomposites prepared via *in-situ* "pH-adjusting" method. Catal Commun 2011;16:11–4.
[42] Zhang X, Qu Z, Yu F, Wang Y. High-temperature diffusion induced high activity of SBA-15 supported Ag particles for low temperature CO oxidation at room temperature. J Catal 2013;297:264–71.

[43] Shukla DB, Pandya VP. Estimation of crystalline phase in ZSM-5 zeolites by infrared spectroscopy. J Chem Technol Biotechnol 1989;44:47–154.
[44] Nayak VS, Chodhary VR. Acid strength distribution and catalytic properties of H-ZSM-5. J Catal 1983;81(1):26–45.
[45] Olson DH, Kokotailo GT, Lawton SL, Meier WM. Crystal structure and structure related properties of ZSM-5. J Phis Shem 1981;85(15):2238–43.
[46] Vosmerikova LN, Barbashin YE, Vosmerikov AV. Synthesis, acidic and catalytic properties of crystalline galloaluminosilicates. Rus J Appl Chem 2000;73 (6):951–6.
[47] Pestryakov AN, Lunin VV. Physicochemical study of active sites of metal catalysts for alcohol partial oxidation. J Mol Catal A: Chem 2000;158:325–9.
[48] Mason MG. Electronic structure of supported small metal clusters. Phys Rev B 1983;27:748–62.
[49] Pestryakov AN, Davydov AA. Study of supported silver states by the method of electron-spectroscopy of diffuse-reflectance. J Electron Spectroscopy Related Phenomena 1995;74:195–9.
[50] Gunnarsson F, Kannisto H, Skoglundh M, Härelind H. Improved low-temperature activity of silver–alumina for lean NO_x reduction – effects of Ag loading and low-level Pt doping. Appl Catal B: Environ 2014;152–153:218–25.
[51] Furusawa T, Seshan K, Lercher JA, Lefferts L, Aika K. Selective reduction of NO to N_2 in the presence of oxygen over supported silver catalysts. Appl Catal B: Environ 2002;37:205–16.
[52] Herzing AA, Kiely CJ, Carley AF, Landon P, Hutchings GJ. Identification of active gold nanoclusters on iron oxide supports for CO oxidation. Science 2008;321:1331–5.
[53] Qu Z, Huang W, Cheng M, Bao X. Restructuring and redispersion of silver on SiO_2 under oxidizing/reducing atmospheres and its activity toward CO oxidation. J Phys Chem B 2005;109:15842–8.
[54] Pestryakov AN, Lunin VV, Kharlanov AN, Bogdanchikova NE, Tuzovskaya IV. Electronic state of gold in supported clusters. Eur Phys J D 2003;24:307–9.
[55] Qi F, Saltsburg H, Flytzani-Stephanopoulos M. Active nonmetallic Au and Pt species on ceria-based water-gas shift catalysts. Science 2003;301:935–8.
[56] Qi F, Deng W, Saltsburg H, Flytzani-Stephanopoulos M. Activity and stability of low-content gold–cerium oxide catalysts for the water–gas shift reaction. Appl Catal B: Environ 2005;56:57–68.
[57] Deng W, Jesus J, Saltsburg H, Flytzani-Stephanopoulos M. Low-content gold-ceria catalysts for the water–gas shift and preferential CO oxidation reactions. Appl Catal A: Gen 2005;291:126–35.
[58] Bogdanchikova N, Pestryakov A, Farias MH, Diaz JA, Avalos M, Navarrete J. Formation of TEM- and XRD-undetectable gold clusters accompanying big gold particles on TiO_2-SiO_2 supports. Solid State Sci 2008;10:908–14.
[59] Pestryakov AN, Lunin VV, Bogdanchikova N, Temkin ON, Smolentseva E. Active states of gold in small and big metal particles in CO and methanol selective oxidation. Fuel 2013;110:48–53.
[60] Pestryakov AN, Davydov AA. Active sites of silver catalysts for methanol oxidation. Kinet Catal 1994;35:279–82.
[61] Tabakova T, Boccuzzi F, Manzoli M, Chiorino A, Andreeva D. Characterization of nanosized gold, silver and copper catalysts supported on ceria. Stud Surf Sci Catal 2005;155:493–500.
[62] Boccuzzi F, Chiorino A, Manzoli M, Andreeva D, Tabakova T, Ilieva L, Iadakiev V. Gold, silver and copper catalysts supported on TiO_2 for pure hydrogen production. Catal Today 2002;75:169–75.